FINAL TECHNICAL REPORT

PILOT PALEOSEISMIC INVESTIGATION OF THE SOUTHERNMOST RODGERS CREEK FAULT, NORTHERN SAN PABLO BAY, CALIFORNIA

Recipient:

Lettis Consultants International, Inc., 1981 N Broadway, Suite 330, Walnut Creek, CA 94596
Phone (825) 482-0360; fax: (925) 482-036; www.lettisci.com

Principal Investigators:
Robert Givler[1] and John Baldwin[1]
Email: givler@lettisci.com; Baldwin@lettisci.com

[1]Lettis Consultants International, Inc.

Contributors:

Nora Lewandowski[1], Matt Huebner[1] Brian Gray[1], and Chris Bloszies[1]

[1]Lettis Consultants International, Inc.

Program Elements II

Keywords:
Quaternary geology, neotectonics, paleoseismology, LiDAR,

U. S. Geological Survey
National Earthquake Hazards Reduction Program
Award Number **G13AP00036**

September 2016

This research was supported by the U.S. Geological Survey (USGS), Department of the Interior, under USGS Awards G13AP00036. The views and conclusions contained in this document are those of the authors and should not be interpreted as necessarily representing the official policies, either expressed or implied, of the U.S. Government.

Award G13AP00036

PILOT PALEOSEISMIC INVESTIGATION OF THE SOUTHERNMOST RODGERS CREEK FAULT, NORTHERN SAN PABLO BAY, CALIFORNIA

Robert Givler[1] and John Baldwin[1]

Principal Investigators:

[1] Lettis Consultants International, Inc., 1981 N Broadway, Suite 330, Walnut Creek, CA 94596
Phone (825) 482-0360; fax: (925) 482-036;
givler@lettisici.com, baldwin@lettisci.com,

ABSTRACT

The timing and recurrence of earthquakes along the Rodgers Creek fault (RCF), including consideration of fault segmentation with the Hayward fault (HF), and are among the most critical issues for reducing uncertainties in probabilistic analyses of seismic hazard in Northern California. The most recent Uniform California Earthquake Rupture Forecast (UCERF 3.0) (Field et al., 2015) assigns a probability of 32% that the HF-RCF will produce an earthquake M≥6.7 in the next 30 years; the highest probability for any San Francisco Bay area fault besides for the San Andreas fault. It is important to note that the probabilistic hazard models (especially time-dependent probabilistic models) are based primarily on slip rate and earthquake timing information derived from just two paleoseismic sites on the central part of the RCF (Schwartz et al., 1992; Hecker et al. 2005). The most recent event (MRE) remains poorly constrained for the southern Rodgers Creek fault (SCRF), which is key to addressing the question regarding the probability of a linked fault rupture between the HF-RSV, as well as the timing of past late Holocene events.

Our pilot paleoseismic study at the Cline Vineyard Site was designed to test whether the stratigraphy at the site records evidence of late Holocene surface ruptures along the SRCF. This site was chosen because of the apparent high sedimentation rate and presence of prominent tectonic geomorphology. The SRCF is mapped as a series of discrete NW-striking fault traces marked by topographic scarps, shutter ridges, deflected drainages, sag ponds, and aligned springs. Two paleoseismic trenches (T-1 and T-2) were excavated across the SCRF. Trench T-1 was excavated across a 1.5-m-high west-facing scarp and northwest-trending swale on the margin of a Holocene terrace (Qt1). The trench exposed folded and tilted late Pleistocene to early Holocene fluvial deposits unconformable overlain by middle to late Holocene colluvium and fine-grained organic-rich overbank deposits. The results from trench T-1 indicate: northwest-striking faults displace the late Pleistocene to late Holocene stratigraphy with a west-side-up dextral displacement and likely form a series of *en echelon* fault strands that step across a late Holocene terrace. We interpret a minimum of three late Holocene events in T-1, although the timing of these events are unconstrained based on a lack of datable material in this trench.

Trench T-2 was excavated across a northwest-trending east-facing scarp that separates Sonoma Volcanics on the west from the Qt1 terrace on the east. T-2 exposed Sonoma Volcanics bedrock overlain by a series of hillslope and scarp-derived (?) colluvial deposits that interfinger with stratified Qt1 fluvial terrace deposits (960 to 805 years BP). Exposures in T-2 suggest that the fault here exhibits primarily strike-slip displacement with a vertical component of east-side-down separation. Multiple scarp-derived colluvial wedge-like deposits are interpreted to record multiple surface rupturing events within the late Holocene (minimum of two events <1,000 years BP).

Based on the initial results of this pilot study, we believe further paleoseismic investigations at the Cline Vineyard Site will yield additional constraints on the paleoseismic history of the SRCF. This study establishes the location of Holocene strands of the SCRF crossing late Holocene fluvial terraces (<1,000 years BP) and results from T-2 exposures suggests a minimum of two surface rupturing events in the last 1,000 yrs. We believe this site has a high potential for success due to the very young site stratigraphy that overlies the active fault zone, abundant possibilities for assessing earthquake timing information and possibly slip-per-event and/or potentially slip rate.

TABLE OF CONTENTS

1.0 INTRODUCTION 1
2.0 TECTONIC SETTING AND REGIONAL GEOLOGY 2
2.1 Paleoseismic Data: Rodgers Creek Fault 2
3.0 APPROACH AND METHODOLOGY 4
4.0 RESULTS 5
4.1 Geologic and Geomorphic Mapping Results 5
4.2 Trench results 5
4.2.1 Trench T-1 5
4.2.2 Trench T-2 6
5.0 DISCUSSION 8
6.0 SUMMARY OF FINDINGS 9
7.0 ACKNOWLEDGEMENTS 11
8.0 REPORTS/ABSTRACTS PUBLISHED 12
9.0 REFERENCES 13

LIST OF TABLES

Table 1 Radiocarbon data for the Cline Vineyard site, Sonoma County, California

LIST OF FIGURES

Figure 1 Regional shaded relief map showing the Cline Vineyard site, past study sites, faults modified from Jennings (1994), and the historical earthquakes of 1969 and 1898 (modified from Givler et al., 2010).

Figure 2 Southern 25 km of the Rodgers Creek Fault showing fault and lineament mapping (Randolph and Caskey, 2001) and previous paleoseismic investigations on the fault. USGS 7.5-minute Quadrangle boundaries shown by dotted line. BVF – Bennette Valley fault (modified from Givler et al., 2010).

Figure 3 Geologic map of the Cline Vineyard Site area (Wagner et al., 2002a; 2002b).

Figure 4 Cline Vineyard Site Geologic Map on a LiDAR base illustrating trench locations excavated as part of this study.

Figure 5 Simplified uninterpreted and interpreted log of the south wall of trench T-1 at the Cline Vineyard Site.

Figure 6 Simplified uninterpreted and interpreted log of the north wall of trench T-1 at the Cline Vineyard Site.

Figure 7 Photomosaic of the Qt1 terrace surface (looking south) with key geologic features annotated.

Figure 8 Simplified interpreted log of trench T-2 (north wall) at the Cline Vineyard Site.

Figure 9 Photomosaic of trench T-2 illustrating the coincidence of the faulting in the trench with the scarp along the western margin of Qt1.

APPENDICES

Appendix A Radiocarbon (C14) results from Beta Analytic, Inc.

1.0 INTRODUCTION

The most recent Uniform California Earthquake Rupture Forecast (UCERF 3.0) (Field et al., 2015) assigns a probability of 32% that the Hayward-Rodgers Creek fault will produce an earthquake M≥6.7 in the next 30 years, the highest probability for any San Francisco Bay Region (SFBR) fault other than the San Andreas fault (Figure 1). The UCERF 3.0 model also increased the number of multi-fault ruptures and a doubling of the probability of events larger than M7.2 from earlier UCERF models (Field et al., 2015). The age of the most recent event (MRE) and recurrence information are important parameters (especially for time-dependent models like UCERF 3.0) for developing rupture scenarios and computing probabilities of future major earthquakes along the Hayward-Rodgers Creek fault (HRCF). Considering the proximity of the SRCF to the heavily populated and urbanized North Bay region, the consequences of a large earthquake on the fault are large (ABAG, 2010). The damage to built structures from the August 2014 Mw 6.0 Napa Earthquake demonstrates how vulnerable this region is to moderate to large earthquake. The lack of significant seismic moment release on the Rodgers Creek fault (RCF) within recorded history suggests that this segment is primed for a large earthquake, up to M7.1 (Lienkaemper et al., 2014). Thus, it is important to regional and local seismic hazard evaluations to understand, as best as possible, the recurrence of large earthquakes on the RCF, as well as on the HRCF system.

However, data used to develop the UCERF 3.0 probabilities for the RCF are based on findings from only two sites along the central part of the RCF (Figure 2; Budding et al., 1991; Schwartz et al., 1992; Hecker et al., 2005). Obtaining additional data from the southern part of the fault is critical to gaining a better understanding of: (1) the timing and recurrence of large paleoearthquakes, (2) potential for multi-segment ruptures with the northern HF (Parsons et al., 2003), and (3) seismic hazard and probabilities of large earthquakes in the rapidly expanding urban area of the northern SFBR.

The Cline Vineyard Site, the focus of this pilot study, provides the key stratigraphic and structural elements to a successful paleoseismic study (Figure 2). As discussed below, this pilot study has yielded initial promising results that, with additional future research, may help to constrain the paleoseismic history of the SRCF.

2.0 TECTONIC SETTING AND REGIONAL GEOLOGY

The RCF includes the central part of an extensive 275-km-long fault system that comprises the Hayward, Rodgers Creek-Healdsburg, and Maacama faults (Figure 1; McLaughlin et al., 2012). The 60-km-long RCF, located between San Pablo Bay and Santa Rosa, California, strikes approximately N35°W, and is characterized by a late Holocene right-lateral slip rate of 6.4 to 10.4 mm/yr (Budding et al., 1991; Schwartz et al., 1992; Hecker et al., 2005).

The RCF has been seismically quiescent historically, despite over 19 **M**>6.0 earthquakes occurring in the Bay Area in the last 150 years (Figures 1 and 2) (WGCEP, 2003). The only moderate to large earthquakes located near the fault were the 1969 **M** 5.6 and 5.7 earthquakes near Santa Rosa (Cloud et al., 1970; Wong, 1991), and the Mare Island event of 1898 (Figure 2). Based on historical accounts for the region, the 1898 earthquake is interpreted by Toppozada et al. (1992) as a **M**6.2 to **M** 6.7 event that may have occurred along the southernmost section of the Rodgers Creek fault. However, the location of the 1898 event remains uncertain due to the lack of definitive supporting information.

During the time since the 1906 San Francisco earthquake on the San Andreas fault, the paucity of moderate to large earthquakes suggests that the SFBR has been in a stress shadow (Harris and Simpson, 1998; Schwartz et al., 2014). Elastic static stress models support a theory in which the 1906 event caused a relaxation of stress on faults of the San Andreas system (Harris and Simpson, 1998). Since the 1989 Loma Prieta earthquake, it is believed that the SFBR is emerging from the 1906-induced stress shadow, and that faults that have been quiescent during the past century, may now once again become more seismically active (Simpson and Reasenberg, 1994; Schwartz et al., 2014; Lienkaemper et al., 2014).

Active creep has been well documented both south and north of the RCF, along the Hayward and the Maacama faults, respectively (Figure 1). Recent creep measurements confirm the SRCF creeps approximately 1.5±0.3 mm/yr (Leinkaemper et al., 2014; McFarland et al., 2016). Recent data from geodetic measurements and from PS-InSAR datasets indicate the fault may be creeping up to or greater than six mm/yr near Santa Rosa, California (Floyd et al., 2009; Funning et al., 2007). The SRCF creeps at the lowest rate and Lienkaemper et al. (2014) suggest the RCF is essentially 90±10% locked and has accumulated enough strain since the MRE to produce a M7.1 earthquake (see below for further discussion of the MRE). These results are consistent with the latest creep monitoring data nearest the site (site RCWC is located 3.6 km to the south), which suggests the fault is creeping slowly (0.3±0.5 mm/yr) (McFarland et al., 2016).

2.1 Paleoseismic Data: Rodgers Creek Fault

Paleoseismic investigations at four sites provide information on the late Holocene slip rate and event chronology for the central and southern parts of the RCF (Figure 2; Budding et. al, 1991; Schwartz et. al, 1992; Hecker et al., 2005; Randolph Loar, 2002; Randolph-Loar et al., 2004). Studies along the central Rodgers Creek fault report an average earthquake recurrence interval of 131 -370 years (Budding et. al, 1991; Schwartz et. al, 1992; Hecker et al., 2005). The studies on the central and southern RCF studies are summarized below:

- **Triangle G Ranch Site** (located ~5.0 km north of the Cline Vineyard site; Figure 2) - Schwartz et al. (1992) identified two events on the central RCF at the Triangle G Ranch that predate the most recent event (MRE), including: (1) the oldest event occurred shortly before 993 to 1193 AD (962-762 yr BP) and (2) a younger event occurred after 993-1193 AD (962-762 yr BP) but before 1275-1413 AD (680 to 542 yr BP). Using non-native pollen and review of historical records, Hecker et

al. (2005) constrain the timing of the most recent earthquake on the RCF to after A.D. 1690 and before A.D. 1715 (234 to 315 yr B P) in trenches at the Triangle G Ranch.

- **Beebe Ranch Site** (located ~5.8 km north of the Cline Vineyard site; Figure 2) **-** Hecker et al. (2005) estimated a buried channel at Beebe Ranch was right-laterally offset a minimum of 2.2 (+1.2, -0.8) m during the MRE, which is similar to but larger than the 2 (+0.3, -0.2) m estimated previously (Budding et al., 1991). Hecker et al. (2005) concluded that the MRE produced 0.25 to 0.4 m of vertical deformation along the fault. They go on to compare the MRE on the RCF to the timing of the last prehistoric ruptures on northern and southern sections of the Hayward fault (A.D. 1640-1776; 315-234 yr BP) and suggest that there is a possibility that an earthquake ruptured both the RCF and Hayward fault across the San Pablo Bay step over.
- **Martinelli Ranch Site** (located 1.3 km north from the site; Figure 2)**–** Located on the northern portion of the SRCF, Randolph-Loar et al. (2004) performed a paleoseismic study at Martinelli Ranch that yielded one surface rupturing event at the site before 1,050-790 cal yr BP and after 10,730-9,550 cal yr BP.
- **Donnell Ranch Site** (located 2 km south of the Cline Vineyard site; Figure 2) **–** Located on the central portion of the SRCF**,** Randolph-Loar (2002) identified one event prior to 6.8 ka, 2 events between 6.8 and 3.7ka and three post 3.7 ka. Randolph-Loar (2002) dated faulted horizons using bulk soil ages (because of a lack of detrital charcoal) and they question the reliability of the bulk ages suggesting that it is possible that the deposits "are all reworked, thus biasing the results towards older events" (p. 6).

The paleoseismic studies at Beebe Ranch and Triangle G Ranch provided constraints on timing and displacement during the MRE and earlier event because these sites have high sedimentation rates and young stratigraphy with datable material. The results from Donnell Ranch recorded fewer events, possibly because the site is located within a small watershed with limited late Holocene deposition (Figure 2). Thus, the Cline Vineyard site was identified as part of this project because (1) the fault is marked by prominent geomorphology and (2) the site has high sedimentation rates marked by a series of recent Holocene fans and fluvial terraces (Figures 3 and 4).

3.0 APPROACH AND METHODOLOGY

Our approach to this pilot paleoseismic study of the SRCF involved two components: (1) geologic/geomorphic mapping, and (2) excavating two paleoseismic trenches across suspected Holocene traces of the SRCF (Figures 2 and 3). The first component used geologic and geomorphic mapping at the Cline Vineyard site to identify suspected Holocene traces of the SRCF. The second component entailed excavating two paleoseismic trenches across suspected Holocene faults to evaluate the age of site stratigraphy and presence of recent surface ruptures on the SRCF.

Geologic and geomorphic mapping was completed over multiple days in the summer of 2014 and 2015 using a combination of aerial photography and LiDAR data. Mapping was conducted on LiDAR base maps using hand-held GPS units to collect waypoint information of key features. The mapping was focused on evaluating past geologic mapping by others (Wagner et al., 2002a; 2002b; Randolph-Loar, 2002) and identifying suspected Holocene traces of the SRCF for future paleoseismic trenches. The preliminary geologic mapping is shown in Figure 4.

After geologic mapping was complete, LCI excavated two paleoseismic trenches across the suspected strands of the SRCF in March of 2015 at the Cline Vineyard Site (Figure 4). During excavation, the trenches were stabilized using hydraulic aluminum shoring according to Cal-OSHA standards. Both the north and south walls of the trenches were cleaned. Geologic deposits exposed in trenches were logged at a scale of 1 inch equals 0.5 meters. The deposits were logged to document the nature of the geologic deposits and any fault contacts exposed in the trenches. The simplified trench logs for trenches T-1 and T-2, and associated field photographs, are included in this report as Figures 5 to 9. Only a partial log of the north wall of trench T-1 is included along the fault zone. Geologic units were delineated based on physical soil properties such as color, consistency, and structure, and differences in grain size such as gravel, sand and fines content, clast composition, and degree of weathering. We assigned broad age ranges to geologic units based on AMS dating, soil development, and cross cutting relationships, although we acknowledge the age designations provided herein are broad and poorly constrained. The seamless photomosaics of the trench walls were developed using structure-from-motion and image-based-modeling techniques using AgiSoft Photoscan and rectified using ArcGIS.

Trenches T-1 and T-2 were reviewed by Dr. David Schwartz (USGS) and Dr. Suzanne Hecker (USGS) on March 17, 2016. Trenches were backfilled on March 18, 2016.

4.0 RESULTS

4.1 Geologic and Geomorphic Mapping Results

The Cline Vineyards Site is located 1.3 km south of Highway 116 in Sonoma, California along the western bank of an unnamed drainage (Figures 2 and 4). At the site, the main trace of the SRCF juxtaposes two members of the Tertiary Sonoma Volcanics (Units Tsvt and Tsvr on the east and west, respectively) (Wagner et. al., 2002a; 2002b; 2011) (Figure 3).

The Quaternary geologic units at the site include Holocene alluvial fan (Units Qfh), Holocene fluvial terraces (Unit Qt), and Holocene colluvial deposits (Unit Qc) (Figure 4). Significant recent erosion is noted by a deeply incised drainage that bisects the Cline Vineyard site. However, incision at the site appears to be historic based on very limited incision 100 meters up stream of trench T-2 (Figure 4). Detailed geologic and geomorphic mapping suggest in the recent past that the Qt1 and Qt2 terraces received regular overbank deposition from the adjacent creek, supplying sediment to record recent co-seismic deformation.

At the Cline Vineyards Site, the SRCF is mapped as a series of discrete fault traces marked by prominent tectonic-related geomorphology, including: northwest-trending topographic scarps, shutter ridges, deflected drainages, sag ponds, and aligned springs (Figure 4) (Herd, 1978; Randolph et al., 2004; Hart, 1992; this study). Detailed geologic mapping, interpretation of LiDAR data, and trench data suggest the SRCF at the site forms primarily a single strand associated with northeast-facing scarps, aligned linear channels, depressions, and bedrock topographic highs (Figure 4). Mapping within the adjacent deeply incised unnamed drainage identified a northwest-striking shear fabric within Tertiary Sonoma volcanics bedrock (Unit Tsvt) coincident along strike with the fault-related geomorphology (Figure 4). To the south, the SRCF is marked by similar prominent tectonic geomorphology indicative of Holocene strike-slip faults (Figures 3 and 4; Hart, 1992; Randolph et al., 2004; Givler et al., 2010).

4.2 Trench results

4.2.1 Trench T-1

Trench T-1 was excavated across a 1.5-m-high west-facing scarp and northwest-trending swale on the margin of a Holocene terrace (referred to hereafter as Qt1) (Figures 4 and 7). The trench crossed the main trace of the SRCF, which is mapped to the north along the eastern margin of a shutter ridge northwest of the Qt1 surface and projecting across the west-facing scarp. Trench T-1 was approximately 25 meters long and up to 3 meters deep. Simplified logs of the south and north walls of trench T-1 are shown in Figures 5 and 6, respectively.

Trench T-1 encountered: (1) Pleistocene claystone (Unit 1); (2) folded and tilted late Pleistocene (?) to Holocene gravel and fine-grained overbank deposits (Units 2-8); (3) Holocene hillslope colluvium (Unit 9); (4) late Holocene scarp-derived colluvium (Unit 10); and (5) massive late Holocene organic-rich fine-grained overbank deposits (Units 8 and 11) (Figures 5 and 6). An angular unconformity separates organic-rich overbank deposits (Unit 11) from underlying folded and faulted late Pleistocene stratigraphy. No detrital charcoal was found in trench T-1 that was deemed suitable for submittal for age dating. Bulk soil samples were collected from the organic-rich unit, but were not submitted due to limited budget.

Two fault zones were identified in trench T-1. Fault zone 1 (FZ1) is a 2-m-wide, northwest-striking, west-dipping, west-side-up fault zone with anastomosing fault splays that flower upsection (Figure 5 and 6).

FZ1 juxtaposes Pleistocene claystone bedrock against Quaternary gravel at the base of the trench. The individual shears are interpreted to displace the base of the massive late Holocene organic-rich, fine-grained overbank deposits by 0.1 to 0.2 m, and terminate upwards into the organic-rich fine grained overbank deposits (Unit 11). We noted the general absence of creep-related fractures in T-1, but acknowledge Unit 11 is heavily bioturbated which may obscure evidence of recent fault rupture and creep-related deformation. No kinematic indicators were found along FZ1 splays, but the flowering and anastomosing nature of the splays suggests strike-slip displacements.

Fault zone 2 (FZ2) is a 2.5-m-wide, northwest-striking, vertical to west-dipping, west-side-up fault zone with several anastomosing splays (Figures 5 and 6). The overall displacement on most FZ2 splays is limited (<0.1 m), but a single steeply dipping splay is interpreted to displace the base of the late Holocene organic-rich deposits (Unit 11) 0.3 to 0.4 m down-to-the-east. No kinematic indicators were found along FZ2 shears. Alternatively, this step could be interpreted as an erosional. This alternative is unlikely because of the coincidence of the underlying FZ2 fault zone and the unconsolidated nature of units 7 and 8, which are unlikely to hold a vertical to slightly overhanging face.

The coincidence of FZ1 with the thalweg of the northwest-trending swale in the Qt1 surface, and FZ2 with the western margin of the sloped formed by the swale is curious and suggests the swale (which is subparallel to FZ1 and FZ2) maybe fault controlled (Figures 5, 6, and 7). Based on the exposures in trench T-1, we interpret a minimum of three events: (1) event 1 is defined by late Holocene scarp-derived colluvium (Unit 10), (2) event 2 folded and faulted the scarp derived colluvium (Unit 10), and (3) event 3 displaced the shallow-organic rich deposits above FZ2 (Unit 11) (Figure 4).

The results from trench T-1 indicate: (1) the northeastern escarpment of trench T-1 represents a fold scarp formed by west-tilted late Pleistocene gravels; (2) the northwest-striking FZ1 and FZ2 faults accommodate west-side-up dextral displacement; (3) the limited displacements on FZ1 and FZ2 suggest that the SRCF steps east locally along the base of a bedrock shutter ridge between trenches T-1 and T-2; and (4) relatively recent (mid-late Holocene ?) surface displacements of late Holocene deposits (Unit 11) have occurred on the SCRF and are recorded in trench T-1.

4.2.2 Trench T-2

Trench T-2 was excavated across a northwest-trending (~N50°W) east-facing scarp that bounds the western margin of the Qt1 terrace (Figures 4, 8, and 9). Trench T-2 was 9.5 m long and 2.2 m deep. Trench T-2 was excavated to evaluate the origin of the northeast-facing topographic escarpment and the presence or absence of earthquake-related scarp-derived colluvium, and to evaluate the site stratigraphy for datable material. The east-facing topographic escarpment forms a 0.5 to 1.0-m-high scarp separating terrace deposits Qt1 on the east from Qt2 on the west (Figure 9). The trench confirmed the presence of an abrupt vertical bedrock contact associated with bedrock shearing, juxtaposition of different volcanic subunits, and displacement of overlying Holocene colluvium and alluvium (Figure 8).

Trench T-2 exposed tuffaceous volcaniclastics (Sonoma Volcanics bedrock) overlain by a series of hillslope and scarp-derived (?) colluvial deposits that onlap a ~1 m step in bedrock (Figure 8). At the eastern end of T-2, colluvial deposits interfinger with stratified Qt1 fluvial terrace deposits. Detrital charcoal collected from the Qt1 deposits yield an age of 960 to 805 years BP (2σ) (960 to 905, 855 to 830, 810 to 805 yr BP) (Table 1; Appendix A), consistent with the youthful (lack thereof) pedogenic development of the deposits.

Trench T-2 encountered two northwest-striking fault zones (F1Z and FZ2) that are coincident with the topographic bedrock escarpment (Figures 8 and 9). FZ1 is a near-vertical fault zone composed of anastomosing shears that flower up from a single strand at the base of the trench. A 30-cm-wide zone of

sheared material (fine-grained sandy silt with sparse pebbles) is interpreted to extend through the overlying colluvium (Unit 11) to the base of the modern soil (Unit 12) suggesting very recent coseismic surface displacement.

Overall, the exposures in T-2 suggest: (1) the fault exhibits primarily strike-slip displacement with a component of east-side-down separation; (2) multiple scarp-derived colluvial wedge-like deposits; (3) FZ1 and FZ2 are coincident with the topographic escarpment separating Qt1 and Qt2 terraces suggesting this break in slope is fault controlled; (4) the presence of ~1 ka stratified Qt1 terrace deposits suggests they likely record recent surface rupturing events; and (5) the presence of detrital charcoal and buried soils can be used in future studies to estimate the age of past surface rupturing earthquakes.

Table 1. Radiocarbon data for the Cline Vineyard Site, Sonoma, California.

Trench	Lab Sample No.[b]	Sample Material	Sample Location (x, y) + depth (m)	Stratigraphic Unit	$\delta^{13}C$	Conventional Radiocarbon age (Yr BP at 1σ)	Calibrated Age (Cal yr BP at 2σ)
T-2 north wall[a]	Beta – 437000	Detrital charcoal	0 m, 0 m 81 cm depth	Unit 9	**-25.3**	1000±30	960 to 905 855 to 830 810 to 805

[a] Sample location is shown on Figure 8

[b] Dating results are included in Appendix A.

5.0 DISCUSSION

Overall, the data collected at the Cline Vineyards Site suggest that the SRCF forms a series of *en echelon* fault strands that record recent surface ruptures (Figure 4). Holocene deformation in trench T-1 includes a combination of co-seismic folding and faulting that is distributed across two fault zones, which matches the limited geomorphic expression of the fault at this trench. The SRCF likely steps southwest from trench T-1 to the fault scarp at the margin of the Qt1 terrace and across this step there are likely a series of small northwest-striking *en echelon* shears beneath the Qt1 terrace surface. These small shears in T-1 may bound the small northwest-striking swale that intersects the Qt1 terrace. Moreover, the eastward tilt of mid-Holocene organic-rich fine grained overbank deposits (Units 7 and 8; Figures 5 and 6) at the east end of the trenches suggest another east-side-down fault may be located just west of the T-1 trench (possibly as part of the step between the faults in T-1 and the scarp on the margin of Qt1).

The angular unconformity in trench T-1 between late Pleistocene to Early Holocene folded and tilted fluvial sands and gravels (Units 2 to 6) and the unconformably overlying Middle to Late Holocene colluvium and fine-grained organic-rich overbank deposits (Units 8, 10, and 11) lead to several key observations. First, the late Pleistocene to Early Holocene sand and gravel deposits were likely deposited when the active channel of the adjacent stream flowed across the Qt1 surface and are sufficiently old to be folded and tilted 20-40° westward. A moderately well-developed argillic horizon in Unit 5 suggests a period of landscape stability before the tilting of these units (Unit 2 to 6). Second, a period of erosion occurred after or during the tilting and folding of these units, which is indicated by the angular unconformity between earlier deposits (e.g., Unit 3) and overlying organic-rich fine-grained overbank deposits (e.g. Unit 11) (Figure 5). Subsequently, a period of deposition is marked by accumulation of the colluvium (Units 9 and 10) and the organic-rich fine-grained deposits (Unit 11), likely after the active channel migrated to its present position and the Qt1 surface began forming as a flood plain. This earlier evidence of faulting appears to be removed by the erosion that formed the angular unconformity. This angular unconformity also suggests considerably more slip has occurred on fault zone FZ1 in trench T-1 than is indicated by the displacement of the overlying fine-grained deposits (Unit 10 and 11).

The trench T-2 exposures confirm the scarp on the western margin of the Qt1 terrace is fault controlled and suggests the boundary between the Qt1 and Qt2 terrace is also fault controlled (Figures 8 and 9), where a 0.5-1.0-m-high muted topographic scarp separates the Qt1 and Qt1 terrace surfaces. This hypothesis is also supported by an auger transect completed across the margin of the Qt-1 terrace (Figure 4), which showed a pronounced step in the top of bedrock and thickening of the colluvium across this scarp. The scarp between the Qt1 and Qt2 surface is also located closer to the active stream channel, which suggest the stratigraphy in the vicinity of this scarp may be coarser, thinly bedded, and contain dateable material (similar to stratigraphy at the eastern end of trench T-2). In addition, the dated detrital charcoal sample from trench T-2 suggests the Qt1 and Qt2 surfaces are very young (<1,000 yrs.). Thus, if the scarp between Qt1 and Qt2 surface is fault controlled it is likely formed by the last several surface rupturing events on the SRCF.

The initial results from the Cline Vineyard site suggest the site has the potential to provide further constraints on the paleoseismic history of the SRCF. This study establishes the location of Holocene strands of the SRCF crossing very young fluvial terraces (<1.0 kya) and interpretation of trench T-2 exposures suggests a minimum of two surface rupturing events in the last 1,000 yrs. We believe this site has a high potential for success because of the very young site stratigraphy that is likely faulted.

6.0 SUMMARY OF FINDINGS

Our pilot paleoseismic investigation at the Cline Vineyard site on the SRCF provides evidence of coseismic surface rupture in the late Holocene. The pilot study consisted of: (1) mapping Holocene fault-related geomorphology and Quaternary geology at the site; and (2) excavation of two paleoseismic trenches across suspected Holocene traces of the SRCF to evaluate possible stratigraphic and structural evidence for coseismic surface rupture related to large earthquakes.

At the Cline Vineyard Site, the SRCF is mapped as a series of discrete fault traces marked by prominent tectonic-related geomorphology, including: northwest-trending topographic scarps, shutter ridges, deflected drainages, sag ponds, and aligned springs (Figure 3) (Randolph et al., 2004; Hart, 1992; this study). Detailed geologic mapping, interpretation of LiDAR data, and trench data suggests the SRCF at the site forms primarily a single strand composed of *en echelon* splays associated with northeast-facing fault scarps, west-facing fold-scarps, aligned linear channels, depressions, and bedrock topographic highs (Figure 3).

Trench T-1 was excavated across a 1.5-m-high west-facing scarp and northwest-trending swale on the margin of a Holocene terrace (Qt1) (Figures 3 and 4). Faulting in T-1 included two northwest-striking steeply dipping fault zones coincident with the mapped trace of the SRCF that that juxtapose different geologic units and flower up towards the ground surface, consistent with a strike-slip style of deformation. The results from trench T-1 indicate: (1) the eastern escarpment of trench T-1 represents a fold scarp formed by west-tilted late Pleistocene gravels; (2) the northwest-striking FZ1 and FZ2 faults accommodate west-side-up dextral displacement; (3) the limited displacements on FZ1 and FZ2 suggest that the SRCF steps west locally along the base of a bedrock shutter ridge between trenches T-1 and T-2; and (4) relatively recent (mid-late Holocene ?) displacements of massive late Holocene basin fill deposits have occurred on the SCRF locally. Based on the exposures in trench T-1, we interpret a minimum of three events: event 1 is defined by late Holocene scarp-derived colluvium (Unit 10), event 2 folded and faulted the scarp derived colluvium (Unit 10), and event 3 displaced the shallow-organic rich deposits above FZ2 (Unit 11) (Figure 4).

Trench T-2 was excavated across a northwest-trending (~N50°W) east-facing scarp that bounds the western margin of the Qt1 terrace (Figures 4, 8, and 9). Trench T-2 exposed Sonoma Volcanics bedrock overlain by a series of hillslope and scarp-derived (?) colluvial deposits interfinger with stratified Qt1 fluvial terrace deposits (960 to 805 years BP) (Appendix A). Trench T-2 encountered two northwest-striking fault zones (FZ1 and FZ2) that are coincident with the topographic bedrock escarpment. FZ1 is a near vertical fault zone composed of anastomosing shears that flower up from a single strand at the base of the trench where different bedrock types are juxtaposed. Overall the exposures in T-2 suggest the following key observations: (1) the fault here exhibits primarily strike-slip displacement with a vertical component of east-side-down separation; (2) multiple scarp-derived colluvial wedge-like deposits suggestive of multiple events within the late Holocene (minimum of two events); (3) the coincidence of FZ1 and FZ2 with a subtle topographic escarpment separating Qt1 and Qt2 terraces; (4) presence of stratified Qt1 terrace deposits that are ~1 kya, and (5) the presence of detrital charcoal and buried soils to estimate the age of past surface-fault ruptures.

Based on the promising results of this pilot study, we believe further paleoseismic investigations at the Cline Vineyard Site will lead to further constraints on the paleoseismic history of the SRCF. Future investigations at the Cline Vineyard Site could include the following: (1) one 10- to 20-m-long trench (PT-1) located 15-20 m south-southwest of test trench T-2 across the topographic escarpment aligned with the fault zone in trench T-2 and separating Qt1 and Qt2 terraces; and (2) a second ~100-m-long trench (PT-2) within the bedrock escarpment and across the Qt1 terrace 150 m north of the test trench T-

2. The proposed trenches are shown on the inset on Figure 4. Trench PT-1 is designed to evaluate the displacement of recent fluvial deposits that bury the fault scarp and are likely displaced. The placement of the trench within fluvial deposits will aid in the recognition of upward fault terminations; potentially scarp-derived colluvium, and possibly displaced strain gauges that could be used for displacement-per-event or slip rate estimates. In addition, PT-1 is located away from nearby trees to reduce bioturbation in the shallow stratigraphy (to the extent possible). Trench PT-2 is designed to evaluate the possibility of scarp-derived colluvial deposits associated with the bedrock escarpment, as well as additional secondary fault strands east of the escarpment offsetting bedded fluvial stratigraphy of Qt1. Our work at Cline Vineyard Site suggests that the SRCF makes a right step between trenches T-1 and T-2, and thus extending trench PT-2 into the Qt1 terrace may encounter a series of *en echelon* secondary faults useful for assessing event stratigraphy.

7.0 ACKNOWLEDGEMENTS

This research was supported by the U.S. Geological Survey's National Earthquake Hazard Reduction Program, under Award No. G13AP00036. The views and conclusions contained in this document are those of the Principal Investigators and should not be interpreted as necessarily representing the official policies, either expressed or implied, of the U.S. Government. We give many thanks Mr. Fred Cline for allowing LCI access and approval to conduct this study. Nora Lewandowski, Matt Huebner, Brian Gray, and Chris Bloszies assisted with the excavation, cleaning, logging and interpretation of the trenches. Thanks to Suzanne Hecker and David Schwartz of the U.S. Geological Survey for reviewing the trenches.

8.0 REPORTS/ABSTRACTS PUBLISHED

Although we plan to present the results of this research at a regional Geological Society of America meeting or Seismological Society of America soon, no research abstracts or report have been presented to discuss the initial findings of the study.

9.0 REFERENCES

Aagaard, B.T., Graves, R.W., Schwartz, D.P., Ponce, D.A, Graymer, R.W., 2010, Ground-Motion Modeling of Hayward Fault Scenario Earthquakes, Part I: Construction of the Suite of Scenarios, BSSA, v.. 100, no. 6, pp. 2927–2944,

Association of Bay Area Governments (ABAG), 2010, Taming natural Disasters: Multi-Jurisdictional Local Hazard Mitigation Plan for the San Francisco Bay Area – 2010 update of 2005 plan, ABAG Publication Number: P09001EQK

Budding, K.E., Schwartz, D.P., and Oppenheimer, D.H., 1991, Slip rate, earthquake recurrence, and seismogenic potential of the Rodgers Creek fault zone, northern California: Initial Results: Geophysical Research Letters, v. 18, no. 3, p. 447-450.

Cloud, W.K., Hill, D.M., Huffman, M.E., Jennings, T.V., McEvily, T.V., Nason, R.D., Steinbrugge, K.V., Tocher, D., Unger, J.D., Youd, T.L., 1970, The Santa Rosa Earthquakes of October, 1969, in Mineral Information Service, California Division of Mines and Geology, v. 23, no. 3, p. 43-63.

Field, E.H., Biasi, G.P., Bird, P., Dawson, T.E., Felzer, K.R., Jackson, D.D., Johnson, K.M., Jordan T.H., Madden, C., Michael, A.J., Milner, K.R., Page, M.T., Parsons, T., Powers, P.M., Shaw, B.E., Thatcher, W.R., Weldon, R.J., Seng, Y., 2015, Long-Term Time-Dependent Probabilities for the Third Uniform California Earthquake Rupture Forecast (UCERF3), Bulletin of the Seismological Society of America, v. 105, no. 2a, p. 511-543.

Floyd, M .A., Funning, G .J., Lipovsky, B ., 2009, Geodetic evidence for creep along the Rodgers Creek and Maacama fault z ones, northern California, AGU F all Meeting, abstract #G23B-0692

Funning, G.J., Burgmann, R., Ferretti, A., Novali, F., Fumagalli, A., 2007, Creep on the Rodgers Creek fault, northern San Francisco Area from a 10 year PS-InSAR dataset, Geophysical Research Letters, v. 34, L19306, doi:10.1029/2007GL030836

Givler, R.W., Baldwin, J., Knudsen, K., 2010, Structural Characterization and Pilot Paleoseismic Investigation of the southernmost Rodgers Creek Fault, Northern San Pablo Bay, California, Final Technical Report for USGS NEHRP Award No. G09AP00022

Harris, R.A., and Simpson, R.W., 1998, Suppression of large earthquakes by stress shadows: a comparison of Coulomb and rate-and-state failure: Journal of Geophysical Research, v. 103, p. 24,439.

Hart, E.W., 1992, Recently active traces of the Rodgers Creek fault, Sonoma County, California: California Department of Conservation, Division of Mines and Geology Open-File Report 92-7, 14 p.

Hayward fault Paleoearthquake Group, 1999, Timing of Paleoearthquakes on the Northern Hayward fault – Preliminary Evidence in El Cerrito, California, U.S. Geological Survey Open-File Report 99-318.

Hecker, S., Pantosti, D.P., Schwartz, D.P., Hamilton, J.C., Reidy, L.M., Powers, T.J. 2005. The most recent large Earthquake on the Rodgers Creek Fault, San Francisco Bay Area. Bulletin of the Seismological Society of America. Vol. 95, No. 3. pp. 844-860, June 2005.

Herd, D.G. 1978. Map of Quaternary faulting along the southern Rodgers Creek fault zone, Glen Ellen, Petaluma River, and Sears Point 7.5 m quadrangles, California, USGS Open File Report. 78-306, map scale 1:24,000

Lienkaemper, J.J., McFarland, F.S., Simpson, R.W., Caskey, S.J., 2014, Using Surface Creep Rate to Infer Fraction Locked for Sections of the San Andreas Fault System in Northern California from Alignment Array and GPS data, Bulletin of the Seismological Society of America, V. 104, no. 6 p. 1-21.

McFarland, F. S., Lienkaemper, J.J., Caskey, S .J., Grove, K., 2016, Data from Theodolite Measurements of Creep Rates on the San Francisco Bay Region Faults, California: 1979 -2007, U.S. Geological Survey Open-file report 2007-1367, 14 p. (updated version 1.8 March 2016)

McLaughlin, R.J., Sarna-Wojcicki, A.M., Wagner, D.L., Fleck, R.J., Langenheim, V.E., Jachens, R.C., Clahan, K., Allen, J. R., Evolution of the Rodgers Creek–Maacama right-lateral fault system and associated basins east of the northward-migrating Mendocino Triple Junction, northern California,

Geosphere, v. 8; no. 2; p. 1-32
Parsons, T., Sliter, R., Geist, E.L,. Jachens, R.C., Jaffe, B.E., Foxgrover, A., Hart, P.E., and McCarthy, J., 2003, Structure and Mechanics of the Hayward–Rodgers Creek Fault Step-Over, San Francisco Bay, California Bulletin of the Seismological Society of America, v. 93, no. 5, pp. 2187–2200,
Randolph, C.E., and Caskey, S.J., 2001 Neotectonics of the southern Rodgers Creek fault, Sonoma County, CA [abs]: EOS Transactions, Annual American Geological Union Meeting, v. 82, no. 47, p. F935.
Randolph-Loar, C.E., 2002, Neotectonics of the Southern Rodgers Creek Fault, Sonoma County, California: Masters Thesis, San Francisco State University, 154 p.
Randolph-Loar, C. E., Witter, R. C., and Lettis, W. R., 2004, Paleoseismic investigation of the southern Rodgers Creek fault, Martinelli Ranch, Sonoma County, CA, Final Technical Report for the U.S. Geological National Earthquake Hazards Program, 14 p.
Schwartz, D.P., Lienkaemper, J.J., Hecker, S., Kelson, K.I., Fumal, T.E., Baldwin, J.N., Seitz, G.G., Niemi, T.M., 2014, The Earthquake Cycle in the San Francisco Bay Region: A.D. 1600-2012, Bulletin of the Seismological Society of America, v., 104, no. 3, p. 1-30
Schwartz, D.P., Pantosti, D., Hecker, S., Okumura, K., Budding, K.E., and Powers, T., 1992, Late Holocene behavior and seismogenic potential of the Rodgers Creek fault zone, Sonoma County, California, Borchardt, G., et al., eds. Proceedings of the Second Conference on Earthquake Hazards in the Eastern San Francisco Bay Area: California Division of Mines and Geology Special Publication 113, p. 393-398.
Simpson, R. W. and P. A. Reasenberg, Earthquake-induced static-stress changes on central California faults, U.S. Geol. Surv. Prof. Pap. 1550-F, 55-89, 1994.
Toppozada, T.R., Bennett, J.H., Hallstrom, C.L., and Youngs, L.G., 1992. 1898 "Mare Island" earthquake at the southern end of the Rodgers Creek fault, m Borchardt, G., and others, eds., Proceedings of the Second Conference on Earthquake Hazards in the Eastern San Francisco Bay Area: California Division of Mines and Geology Special Publication 113, p. 385-392.
Wagner, D.L., Rice, S.J., Bezore, S.P., Randolph-Loar, C.E., Allen, J.R. and Witter, R.C., 2002a, Geologic map of the Petaluma River 7.5' Quadrangle, Marin and Sonoma counties, California: A digital database: California Geological Survey website, http://www.conservation.ca.gov/-cgs/rghm/rgm/preliminary_geologic_maps.htm
Wagner, D.L., Rice, S.J., Bezore, S.P., Randolph-Loar, C.E., Witter, R.C., and Allen, J.R., 2002b, Geologic map of the Sears Point 7.5' Quadrangle, Sonoma, Solano, and Napa Counties, California: A digital database: California Geological Survey website, http://www.conservation.ca.gov/-cgs/rghm/rgm/preliminary_geologic_maps.htm
Wagner, D.L., Saucedo, G.J., Clahan, K.B., Fleck, R.J., Langenheim, V.E., McLaughlin, R.J., Sarna-Wojcicki, A.M., Allen, J.R., Deino, A.L., 2011, Geology, geochronology, and paleogeography of the southern Sonoma volcanic field and adjacent areas, northern San Francisco Bay region, California, Geosphere, v. 7, no 3, p. 658-683.
Wong, I.G., 1991, Contemporary seismicity, active faulting and seismic hazards of the Coast Ranges between San Francisco Bay and Healdsburg, California: Journal of Geophysical Research, v. 96, no. B12, p.19,891-19,904.
Working Group on California Earthquake Probabilities, 2008, The Uniform California Earthquake Rupture Forecast, Version 2 (UCERF 2). 2007. U.S. Geological Survey Open-File Report 2007-1437 and California Geological Survey Special Report 203 [http://pubs.usgs.gov/of/2007/1437/]

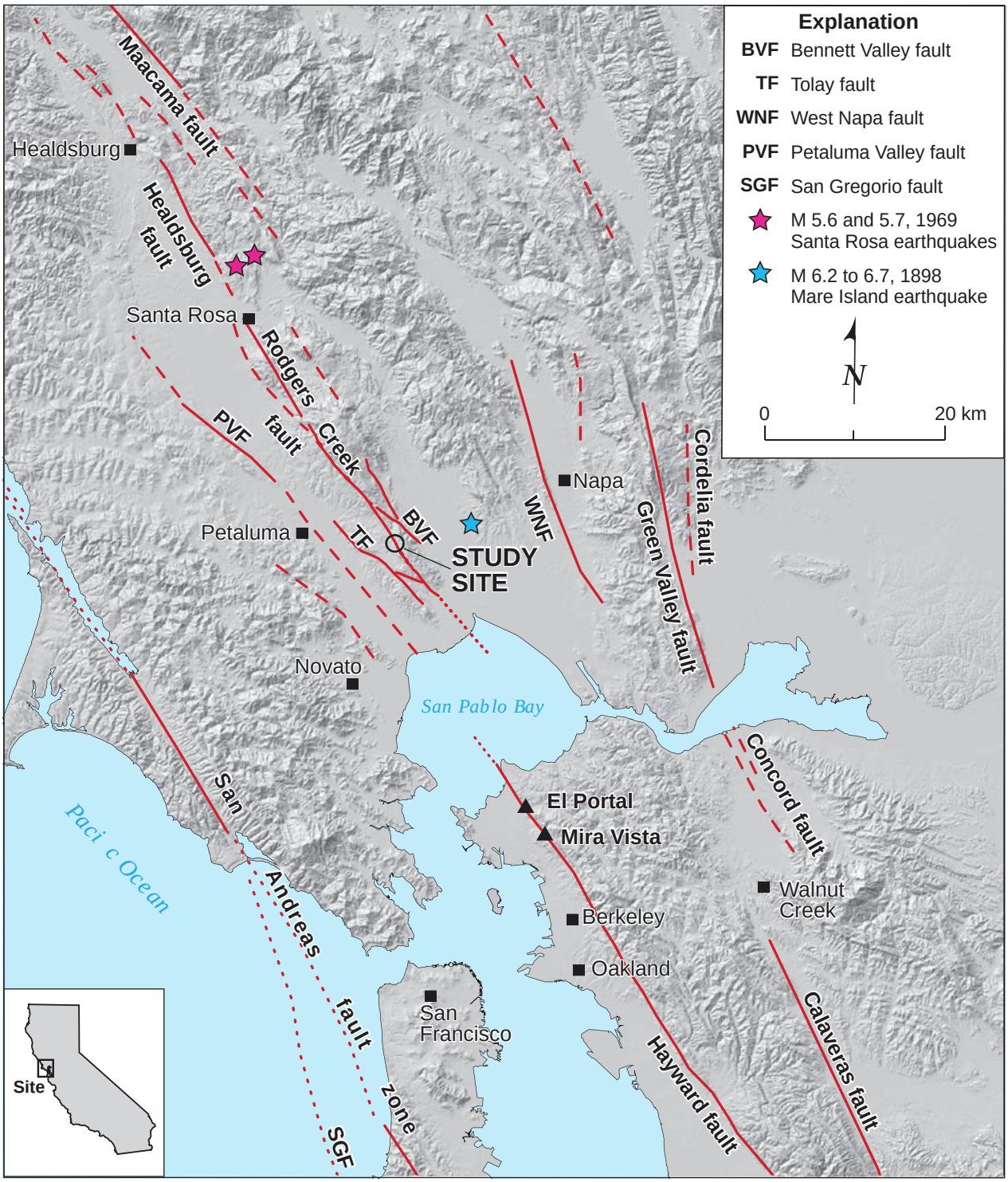

Figure 1. Regional shaded relief map showing the Cline Vineyard Site and past study sites, faults modified from Jennings (1994), and the historical earthquakes of 1969 and 1898 (modified from Givler et al., 2010).

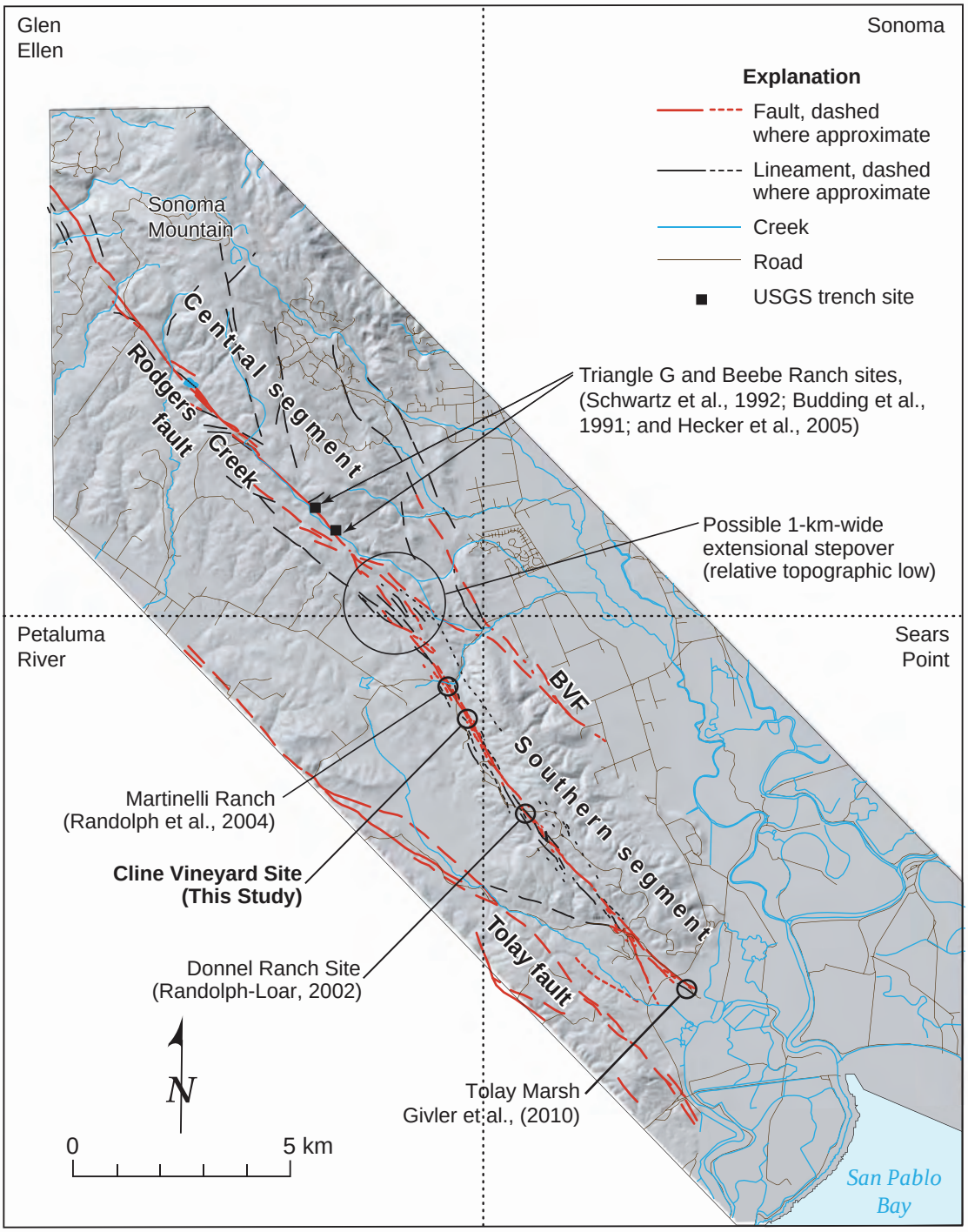

Figure 2. Southern 25 km of the Rodgers Creek fault showing fault and lineament mapping (Randolph and Caskey, 2001) and previous paleoseismic investigations on the fault. USGS 7.5-minute Quadrangle boundaries shown by dotted line. BVF-Bennett Valley fault (modi ed from Givler et al., 2010).

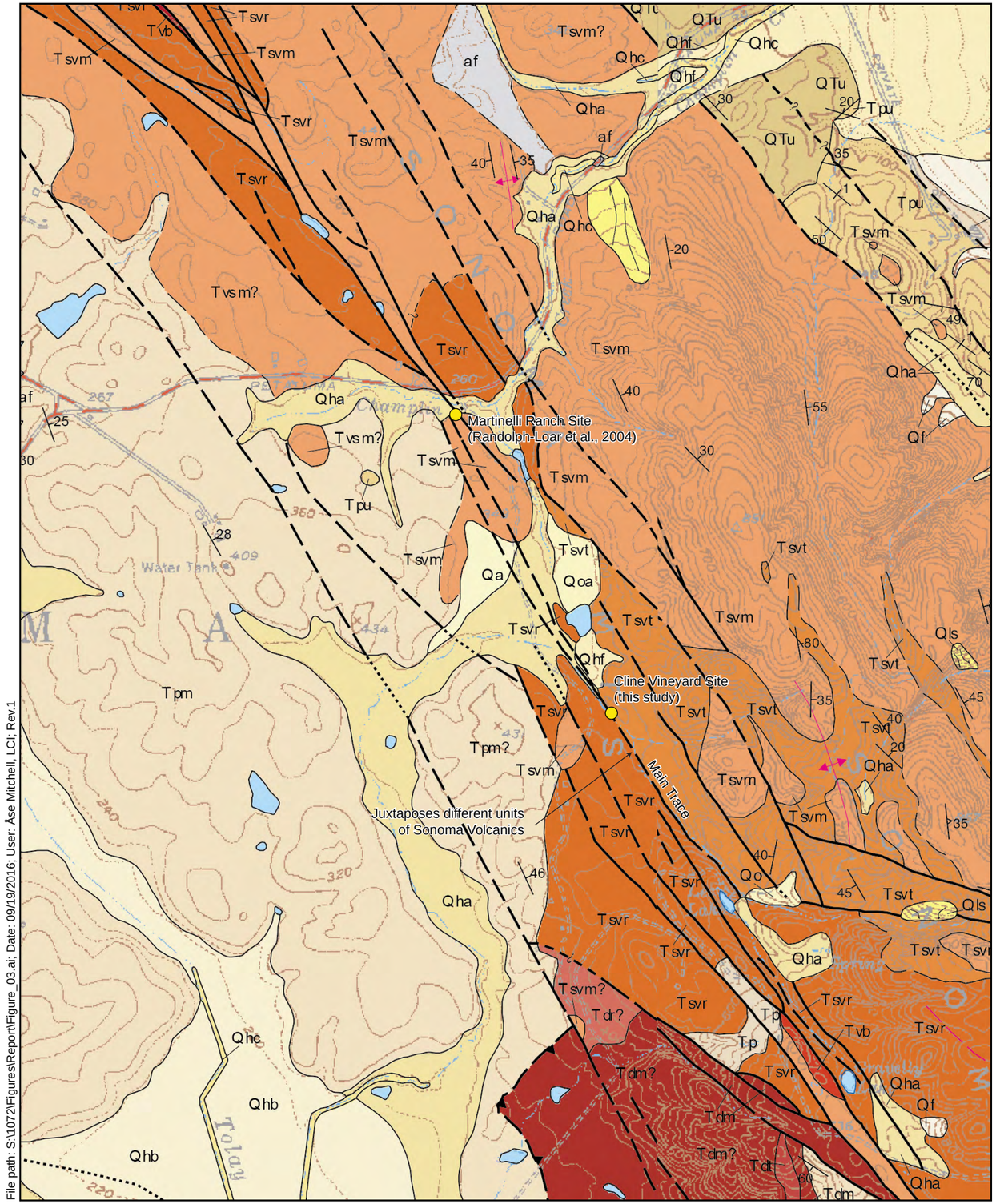

Geologic Units:

af	Artificial fill
Qhc	Late Holocene to modern (<150 years) stream channel deposits in active, natural stream channels. Consists of loose alluvial sand, gravel, and silt.
Qhf	Holocene alluvial fan deposits. Sand, gravel, silt, and clay deposited by streams emanating from canyons onto alluvial valley floors. Sediment is poorly to moderatly sorted and bedded.
Qha	Holocene alluvium, undivided. Alluvium deposited on fans, terraces, or in basins. Sand, gravel, and silt that are poorly sorted.
Qhb	Holocene basin deposits. Fine-grained alluvium with horizontal stratification. May have interbedded peat.
Qf	Latest Pleistocene (<30,000 years) to Holocene alluvial fan deposits. Sand, gravel, silt and clay mapped on gently sloping, fan-shaped, relatively undissected alluvial surfaces.
Qa	Latest Pleistocene to Holocene alluvium, undivided. Flat, relatively undissected fan, terrace, and basin deposits.
Qls	Landslides. Includes debris flow and block slump landslides. Arrows show the direction of movement.
Qoa	Early to late Pleistocene alluvial deposits, undivided. Alluvial fan, stream terrace, basin, and channel deposits. Topography is gently rolling with with little or no original alluvial surfaces preserved; moderately to deeply dissected.
QTu	Gravel, sand, reworked tuff and clay of unknown age. Sediments derived mostly from the Sonoma Volcanics.

Petaluma Formation:

Tp (Trt, Tpu, Tpm, Tpl)

Tpu- Upper Petaluma Fm. Massive, well sorted sandstone, siltstone, and conglomerate. Conglomerate is rich in laminated siliceous shale (Monterey Fm.) fragments and Tertiary volcanics, with Franciscan clasts. The Roblar Tuff (Trt), dated at 6.26 Ma (Robert Fleck, written communication, 2002) is interbedded with the Upper Petaluma.

Tpm- Middle Petaluma Fm. Siltstone with interbedded conglomerate. Clasts in conglomerate are mostly pebbles derived from the Franciscan, but clasts of Cretaceous and Tertiary sandstone as well as Tertiary volcanics are present. Minor siliceous shale fragments from the Monterey Formation are also present.

Tpl- Lower Petaluma Fm. Dominantly bluish to green clayey siltstone and shale with interbeds of silicified tuff, siliceous limestone, lignite, and rare bituminous chert. Laminated siltstone near the base in places. Localities near Tolay Creek and elsewhere have yielded transitional marine and estuarine horizons in a predominantly lacustrine and fluvial deposit

Sonoma Volcanics:

Tsv (Tsvm, Tsvt, Tsvr)

Tsvm- Mafic flows and breccias. Andesite and basaltic andesite. Age range is 7.28 to 3.80 Ma (Youngman, 1989).

Tsvt- Silicic tuff and interbedded tuffaceous sediments. Interbedded sand and gravel is similar to the MIddle Petaluma Formation.

Tsvr- Rhyolitic to dacitic flows, breccias, and sediments. Pink, white, gray, brown flow banded rhyolite in flows, debris flows and breccia. Interbeds of sand, gravel, and tuff. Dates (Ar/Ar) range from 7.36 to 8.11 Ma (Randolph-Loar, 2002; Youngman, 1989; Fox and others,1985).

Donnell Ranch Volcanics (1989):

Tdm, Tdt, Tdr

Tdm- Mafic volcanics including mafic flows and breccia. mostly basalt and basaltic andesite flows and breccia. Scoria is abundant locally.

Tdt- Light colored tuff interbedded with mafic volcanics.

Tdr- Rhyolite to dacite flows and tuff. A radiometric date of 9.56 Ma on the rhyolite was reported by Fox and others (1985). This unit is called the Rhyolite of St. Helena by Weaver (1949).

0 .5 1 Miles

Source: Wagner et al. 2002 geologic mapping of the Sears Point and Petaluma River 7.5' quadrangles

File path: S:\1072\Figures\Report\Figure_03.ai; Date: 09/19/2016; User: Åse Mitchell, LCI; Rev.1

Figure 3. Geologic Map of the Cline Vineyard Site Area (Wagner et al., 2002 a,2002 b)

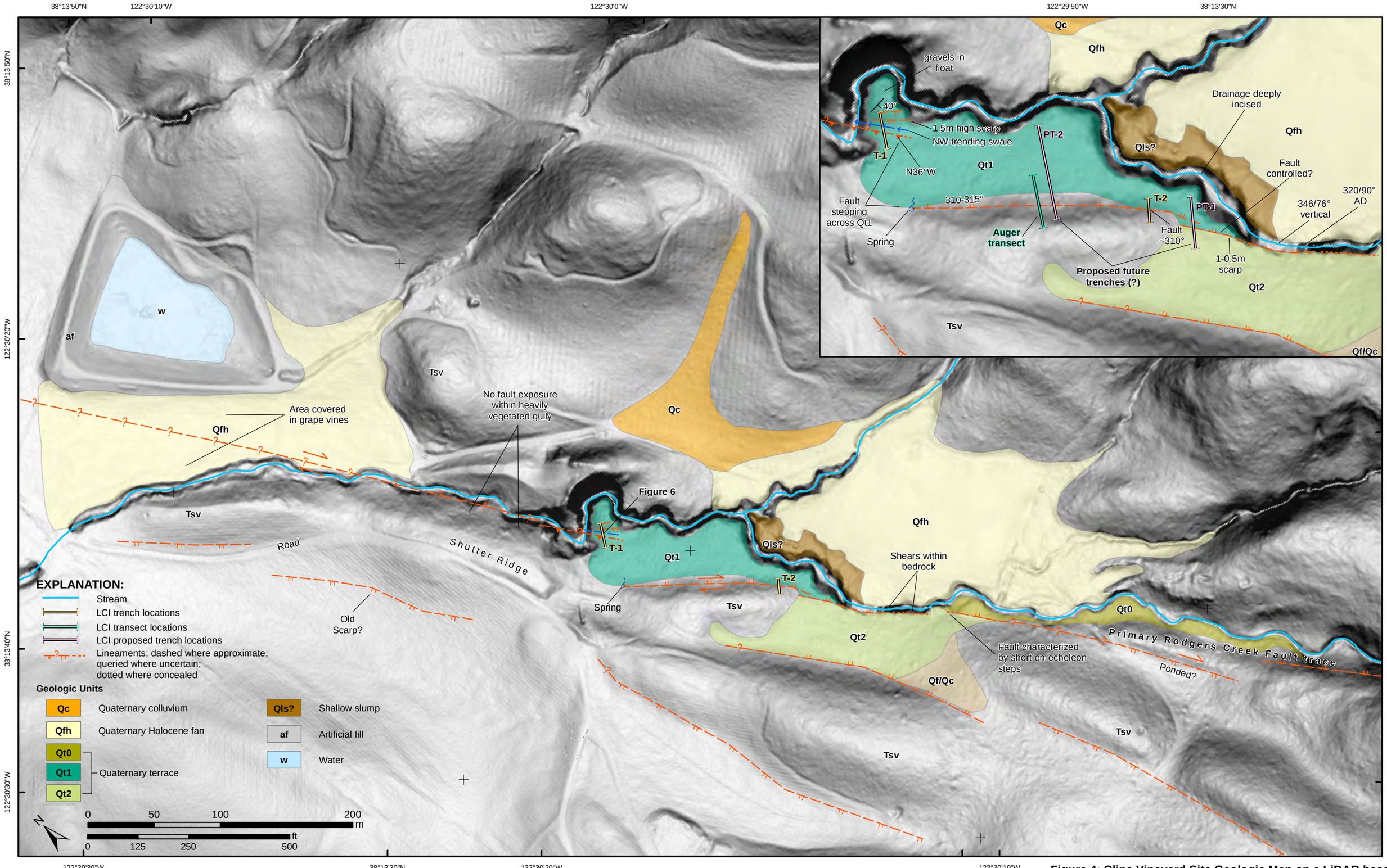

Figure 4: Cline Vineyard Site Geologic Map on a LiDAR base illustrating trench locations excavated as part of this study

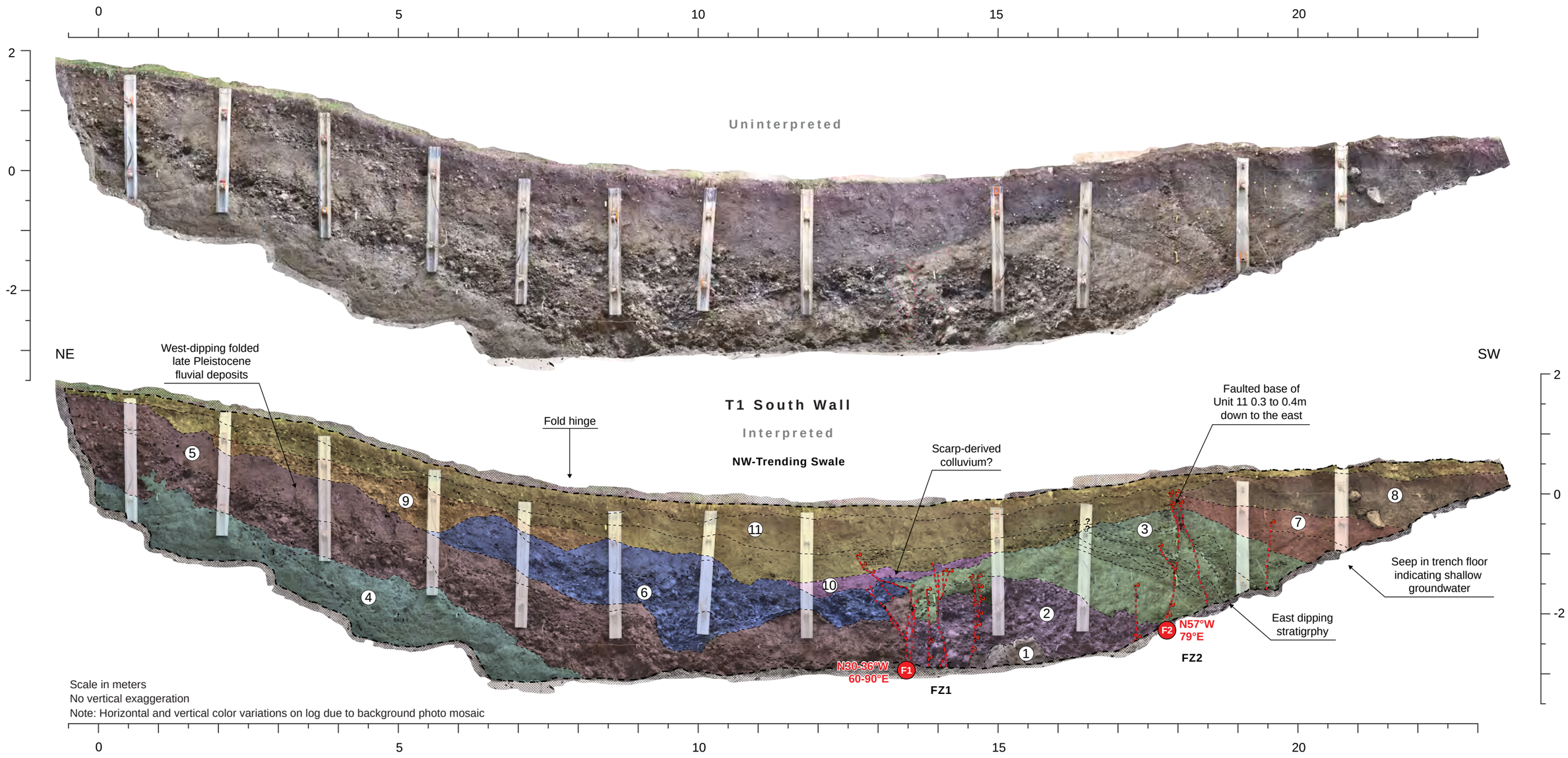

Explanation:

Fault splays; dashed where approximate; queried where uncertain

Geologic contact

Ground Surface

Area of Wall Covered by Trench Shore

N57°W 79°E Fault Attitude

Trench base and corners

Geologic Units:

Unit 11 - Late Holocene organic rich fine grained overbank deposits

Unit 10 - Late Holocene scarp-derived colluvium?

Unit 9 - Late to Mid-Holocene hillslope colluvium

Unit 8 - Late to Mid-Holocene organic rich fine-grained overbank and sag pond (?) deposits

Unit 7 - Early Holocene (?) fine-grained overbank deposits

Unit 6 - Early Holocene gravel, sand and silt (gravel #2)

Unit 5 - Early Holocene to Late Pleistocene gravel and silt

Unit 4 - Late Pleistocene massive gravel and silt (gravel #1)

Unit 3 - Late Pleistocene fine-grained well bedded sand, silt and gravel

Unit 2 - Late Pleistocene folded gravels

Unit 1 - Pleistocene claystone bedrock

Figure 5. Simplified uniterpreted and interpreted log of the south wall trench T-1 at the Cline Vineyard Site

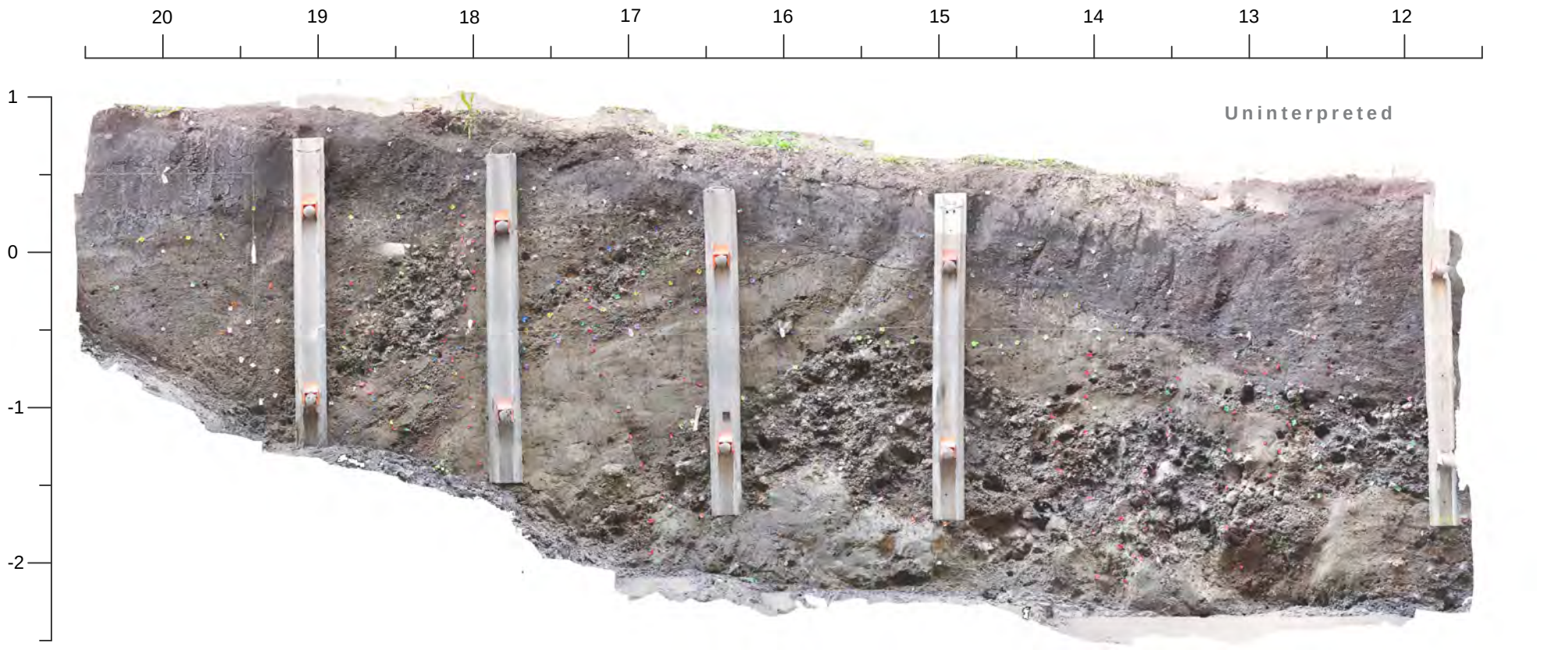

T1 North Wall

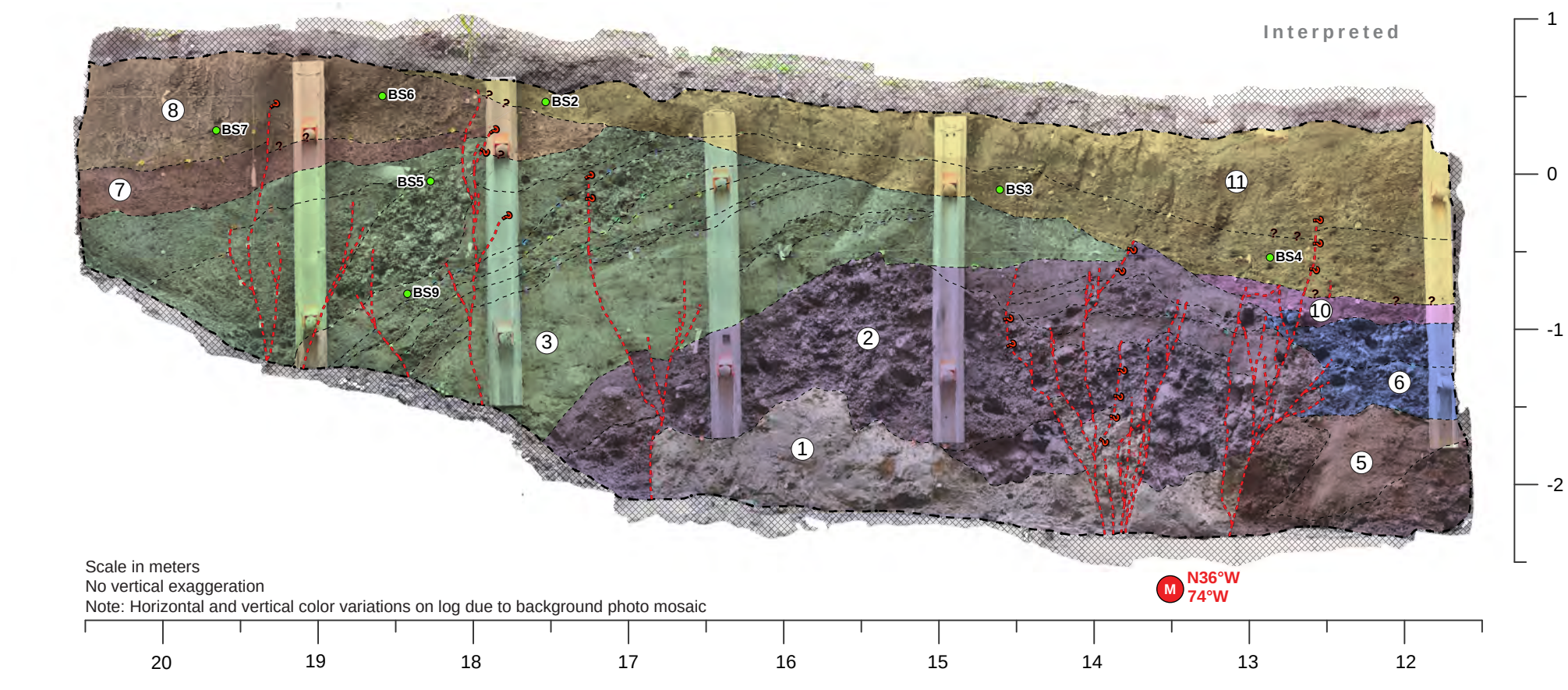

Explanation:

- Fault splays; dashed where approximate; queried where uncertain
- Geologic contact
- Ground Surface
- M N36°W 74°W — Fault Attitude
- Trench base and corners
- Area of Wall Covered by Trench Shore
- BS7 — Bag sample

Geologic Units:

- 11 — **Unit 11 -** Late Holocene organic rich fine grained overbank deposits
- 7 — **Unit 7 -** Early Holocene (?) fine-grained overbank deposits
- 3 — **Unit 3 -** Late Pleistocene fine-grained well bedded sand, silt, and gravel
- 10 — **Unit 10 -** Late Holocene scarp-derived colluvium?
- 6 — **Unit 6 -** Early Holocene gravel, sand and silt (gravel #2)
- 2 — **Unit 2 -** Late Pleistocene folded gravels
- 8 — **Unit 8 -** Late to Mid-Holocene organic rich fine-grained overbank and sag pond (?) deposits
- 5 — **Unit 5 -** Early Holocene to Late Pleistocene gravel and silt
- 1 — **Unit 1 -** Pleistocene claystone bedrock

Figure 6. Simplified uniterpreted and interpreted log of the nouth wall trench T-1 at the Cline Vineyard Site

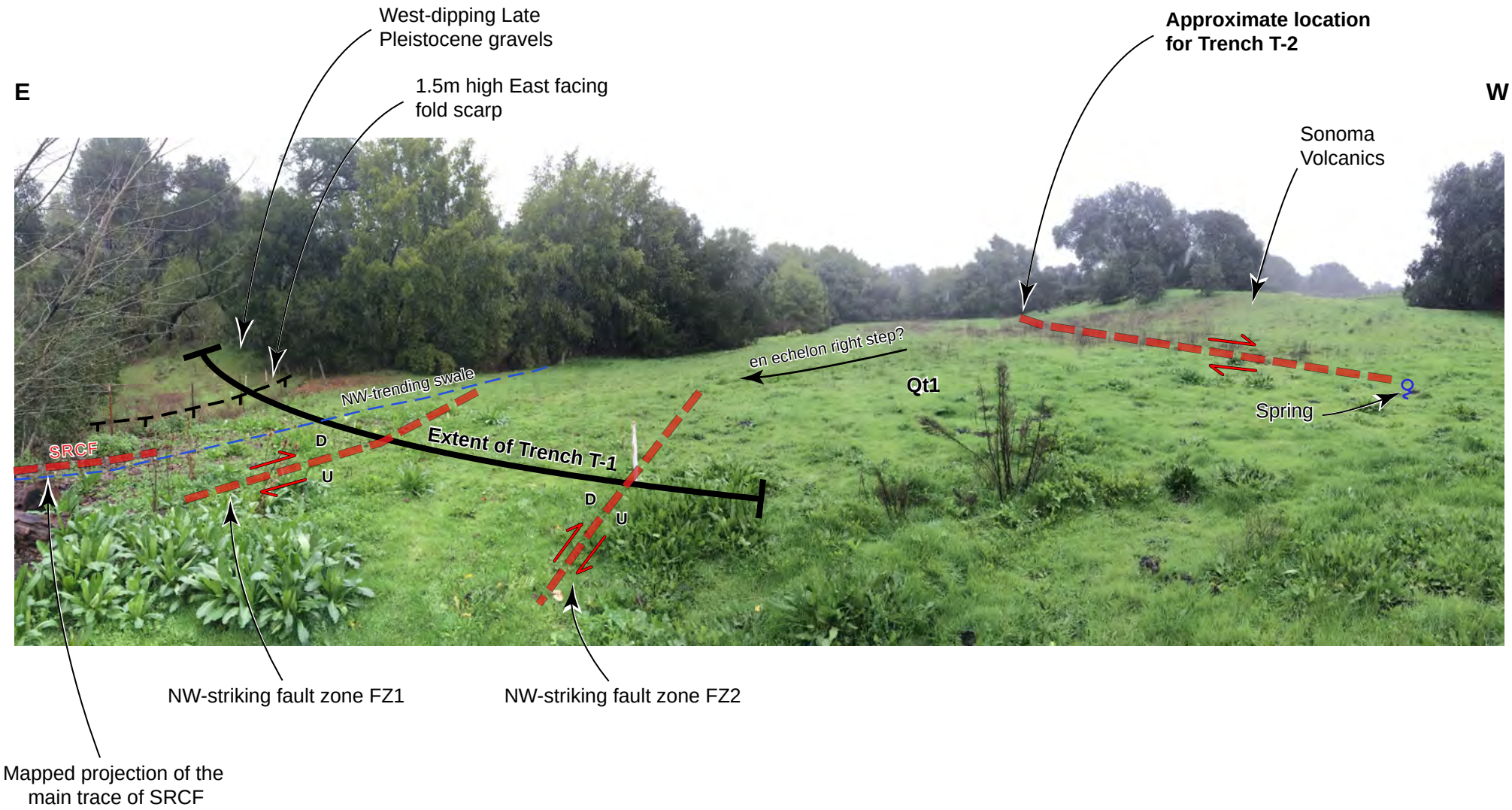

Figure 7. Photomosaic of the Qt1 terrace surface looking south with key geologic features annotated.

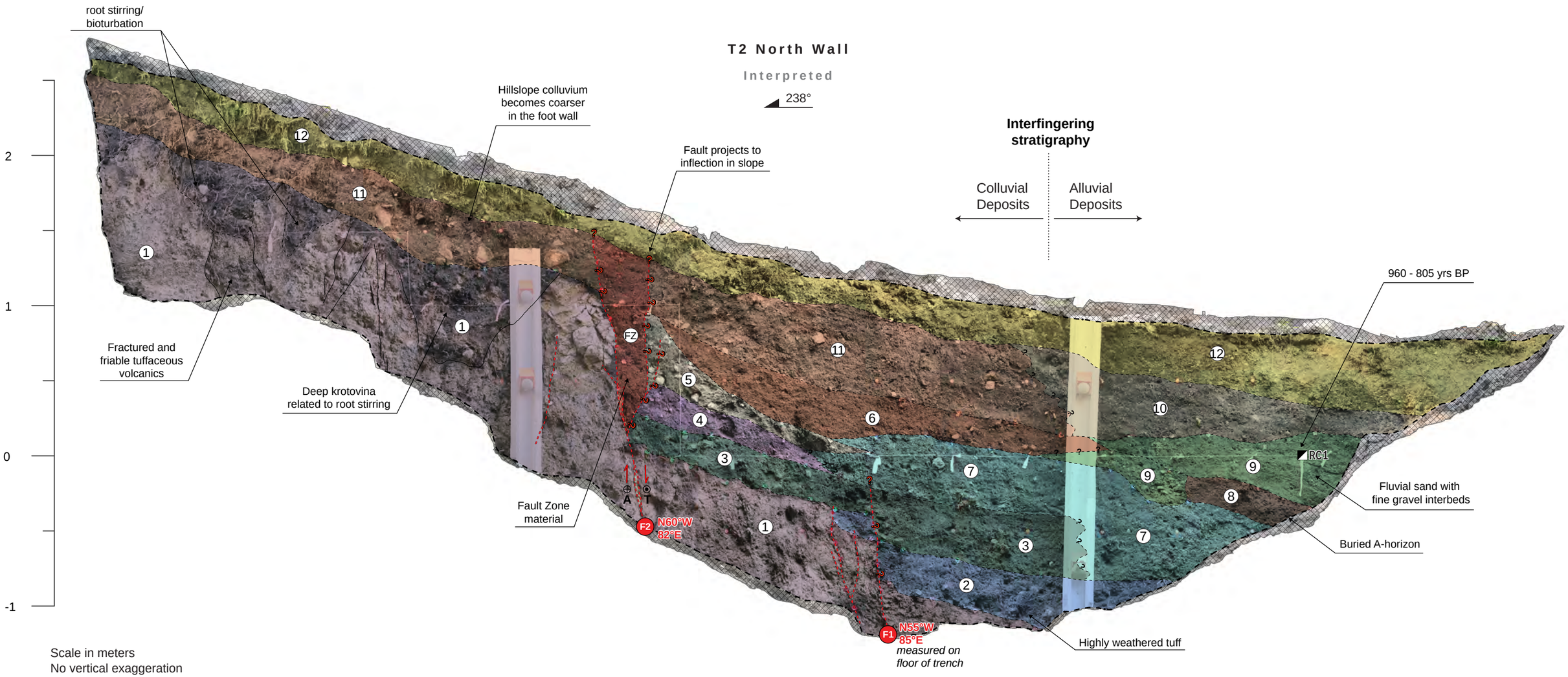

Scale in meters
No vertical exaggeration
Note: Horizontal and vertical color variations on log due to background photo mosaic

8 7 6 5 4 3 2 1 0 -1

Explanation:

Fault splays; dashed where approximate; queried where uncertain

F2 N60°W 82°E Fault Attitude

Geologic contact

RC1 Radiocarbon Sample *Location and designation*

Trench base and corners

Ground Surface

Area of Wall Covered by Trench Shore

Geologic Units:

1 **Unit 1** - Sonoma Volcanics Tuff

2 **Unit 2** - Highly weathered Sonoma Volcanics tuff

3 **Unit 3** - Silty soil with coarse angular gravel (Basal Colluvium or Alluvium)

4 **Unit 4** - Silty sand with fine gravel (scarp(?) colluvium or alluvium)

5 **Unit 5** - Coarse colluvium (Scarp derived?)

6 **Unit 6** - Fine-grained silty sand with minor gravel clasts

7 **Unit 7** - Massive silty soil with minor gravel clasts

8 **Unit 8** - Buried A-horizon formed within Unit 7 (locally discontinuous)

9 **Unit 9** - Fluvial sands, silt and gravels well-bedded throughout

10 **Unit 10** - Massive sandy silt with minor gravel; (A-B-horizon? formed within over bank deposits?)

11 **Unit 11** - Coarse hill slope colluvium (fines away from the fault scarp)

12 **Unit 12** - A-horizon developed in colluvium/ alluvium

FZ **Unit FZ** - Fault Zone material

Figure 8. Simplified interpreted log of trench T-2 at the Cline Vineyard Site

Figure 9. Photomosaic of trench T-2 illustrating the coincidence of the faulting in the trench with the scarp along the western margin of Qt1.

Appendix A:

Radiocarbon (C14) results from Beta Analytic, Inc.

Beta Analytic Inc.
4985 SW 74 Court
Miami, Florida 33155 USA
Tel: 305 667 5167
Fax: 305 663 0964
Beta@radiocarbon.com
www.radiocarbon.com

Consistent Accuracy . . .
. . . Delivered On-time

Darden Hood
President

Ronald Hatfield
Christopher Patrick
Deputy Directors

May 16, 2016

Ms. Nora Lewandowski
Lettis Consultants International
1981 N. Broadway
Walnut Creek, CA 94506

RE: Radiocarbon Dating Result For Sample RC1

Dear Ms. Lewandowski:

Enclosed is the radiocarbon dating result for one sample recently sent to us. The report sheet contains the Conventional Radiocarbon Age (BP), the method used, material type, and applied pretreatments, any sample specific comments and, where applicable, the two-sigma calendar calibration range. The Conventional Radiocarbon age has been corrected for total isotopic fractionation effects (natural and laboratory induced).

All results (excluding some inappropriate material types) which fall within the range of available calibration data are calibrated to calendar years (cal BC/AD) and calibrated radiocarbon years (cal BP). Calibration was calculated using the one of the databases associated with the 2013 INTCAL program (cited in the references on the bottom of the calibration graph page provided for each sample.) Multiple probability ranges may appear in some cases, due to short-term variations in the atmospheric ^{14}C contents at certain time periods. Looking closely at the calibration graph provided and where the BP sigma limits intercept the calibration curve will help you understand this phenomenon.

Conventional Radiocarbon Ages and sigmas are rounded to the nearest 10 years per the conventions of the 1977 International Radiocarbon Conference and consistent with all past Beta Analytic radiocarbon dates. When counting statistics produce sigmas lower than +/- 30 years, a conservative +/- 30 BP is cited for the result. The reported d13C was measured separately in an IRMS (isotope ratio mass spectrometer). It is NOT the AMS d13C which would include fractionation effects from natural, chemistry and AMS induced sources.

All work on this sample was performed in our laboratories in Miami under strict chain of custody and quality control under ISO/IEC 17025:2005 Testing Accreditation PJLA #59423 accreditation protocols. Sample, modern and blanks were all analyzed in the same chemistry lines by professional technicians using identical reagents and counting parameters within our own particle accelerators. A quality assurance report is posted to your directory for each result.

The cost of the analysis was charged to the credit card provided. Thank you. As always, if you have any questions or would like to discuss the results, don't hesitate to contact me.

Sincerely,

Darden Hood

Digital signature on file

BETA ANALYTIC INC.
DR. M.A. TAMERS and MR. D.G. HOOD
4985 S.W. 74 COURT
MIAMI, FLORIDA, USA 33155
PH: 305-667-5167 FAX:305-663-0964
beta@radiocarbon.com

REPORT OF RADIOCARBON DATING ANALYSES

Ms. Nora Lewandowski — Report Date: 5/16/2016

Lettis Consultants International — Material Received: 5/6/2016

Sample Data	Measured Radiocarbon Age	d13C	Conventional Radiocarbon Age(*)
Beta - 437000	1000 +/- 30 BP	-25.3 o/oo	1000 +/- 30 BP

SAMPLE : RC1
ANALYSIS : AMS-Standard delivery
MATERIAL/PRETREATMENT : (charred material): acid/alkali/acid
2 SIGMA CALIBRATION : Cal AD 990 to 1045 (Cal BP 960 to 905) and Cal AD 1095 to 1120 (Cal BP 855 to 830) and Cal AD 1140 to 1145 (Cal BP 810 to 805)

Dates are reported as RCYBP (radiocarbon years before present, "present" = AD 1950). By international convention, the modern reference standard was 95% the 14C activity of the National Institute of Standards and Technology (NIST) Oxalic Acid (SRM 4990C) and calculated using the Libby 14C half-life (5568 years). Quoted errors represent 1 relative standard deviation statistics (68% probability) counting errors based on the combined measurements of the sample, background, and modern reference standards. Measured 13C/12C ratios (delta 13C) were calculated relative to the PDB-1 standard.

The Conventional Radiocarbon Age represents the Measured Radiocarbon Age corrected for isotopic fractionation, calculated using the delta 13C. On rare occasion where the Conventional Radiocarbon Age was calculated using an assumed delta 13C, the ratio and the Conventional Radiocarbon Age will be followed by "*". The Conventional Radiocarbon Age is not calendar calibrated. When available, the Calendar Calibrated result is calculated from the Conventional Radiocarbon Age and is listed as the "Two Sigma Calibrated Result" for each sample.

CALIBRATION OF RADIOCARBON AGE TO CALENDAR YEARS

(Variables: C13/C12 = -25.3 o/oo : lab. mult = 1)

Laboratory number	**Beta-437000 : RC1**
Conventional radiocarbon age	**1000 ± 30 BP**
Calibrated Result (95% Probability)	**Cal AD 990 to 1045 (Cal BP 960 to 905)** **Cal AD 1095 to 1120 (Cal BP 855 to 830)** **Cal AD 1140 to 1145 (Cal BP 810 to 805)**
Intercept of radiocarbon age with calibration curve	Cal AD 1020 (Cal BP 930)
Calibrated Result (68% Probability)	Cal AD 1015 to 1030 (Cal BP 935 to 920)

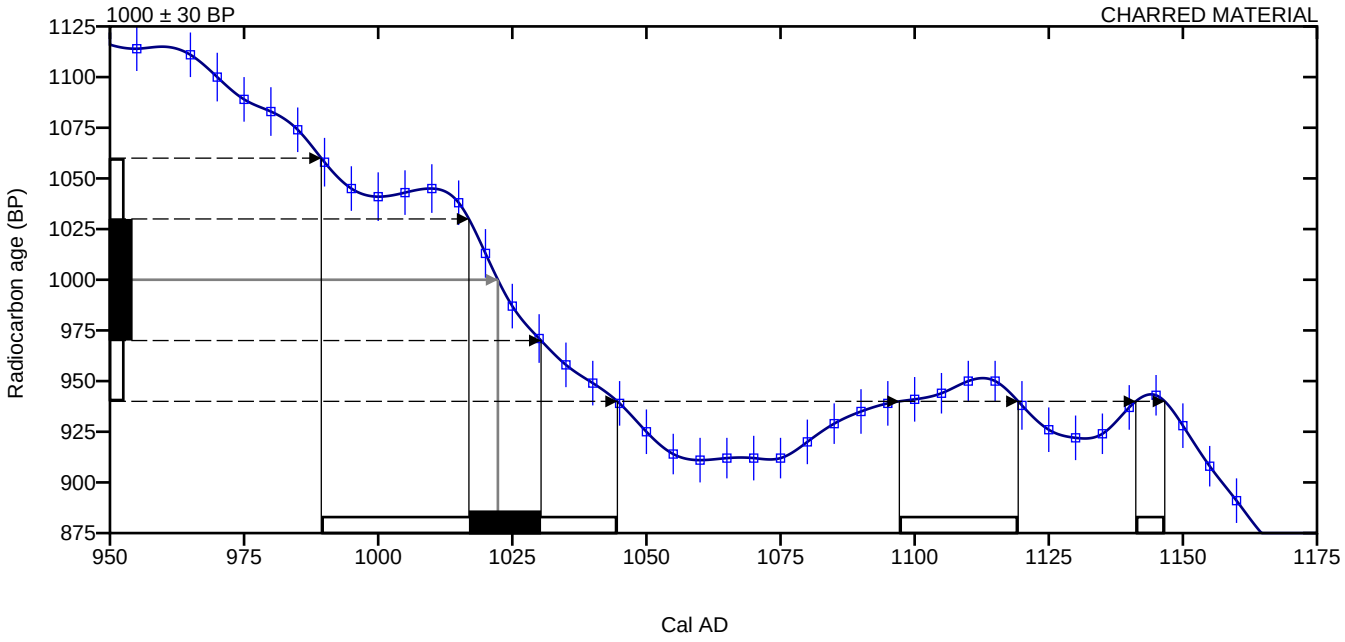

Database used

INTCAL13

References

Mathematics used for calibration scenario

A Simplified Approach to Calibrating C14 Dates, Talma, A. S., Vogel, J. C., 1993, Radiocarbon 35(2):317-322

References to INTCAL13 database

Reimer PJ et al. IntCal13 and Marine13 radiocarbon age calibration curves 0– 50,000 years cal BP. Radiocarbon 55(4):1869– 1887., 2013.

Beta Analytic Radiocarbon Dating Laboratory
4985 S.W. 74th Court, Miami, Florida 33155 • Tel: (305)667-5167 • Fax: (305)663-0964 • Email: beta@radiocarbon.com